MICROWAVE-ASSISTED SOLVOTHERMAL SYNTHESIS OF CUBIC FERRITE (MFE_2O_4, M = Mn, Zn, Cu AND Ni) NANOCRYSTALS AND THEIR MAGNETIC PROPERTIES

A. PHURUANGRAT[a,*], B. KUNTALUE[b], P. DUMRONGROJTHANATH[c], T. THONGTEM[c,d], S. THONGTEM[d,e]
[a]*Department of Materials Science and Technology, Faculty of Science, Prince of Songkla University, Hat Yai, Songkhla 90112, Thailand*
[b]*Electron Microscopy Research and Service Center, Faculty of Science, Chiang Mai University, Chiang Mai 50200, Thailand*
[c]*Department of Chemistry, Faculty of Science, Chiang Mai University, Chiang Mai 50200, Thailand*
[d]*Materials Science Research Center, Faculty of Science, Chiang Mai University, Chiang Mai 50200, Thailand*
[e]*Department of Physics and Materials Science, Faculty of Science, Chiang Mai University, Chiang Mai 50200, Thailand*

MFe_2O_4 (M = Mn, Zn, Cu and Ni) nanoparticles were synthesized by a microwave-assisted solvothermal method. The as-synthesized MFe_2O_4 nanoparticles were characterized by X-ray diffraction, Fourier transform infrared spectroscopy and transmission electron microscopy. The magnetic properties were examined by vibrating sample magnetometer (VSM). XRD patterns show cubic ferrite MFe_2O_4 (M = Mn, Zn, Cu and Ni) with a spinel-type structure. FTIR spectra show the vibration band at ~600–585 cm^{-1} of stretching mode of Fe–O and at ~407–406 cm^{-1} of stretching mode of M–O. The VSM analysis revealed ferromagnetic hysteresis in the field range of ±1000 Oe and ±3000 Oe for the $NiFe_2O_4$ and $MnFe_2O_4$ samples, respectively, whereas the superparamagnetic behavior for the $ZnFe_2O_4$ and $CuFe_2O_4$ samples.

(Received March 1, 2018; Accepted June 15, 2018)

Keywords: Metal ferrite, Microwave-assisted solvothermal method, Magnetic materials

1. Introduction

MFe_2O_4 (M = Mn, Co, Ni, Zn, Mg, etc.) spinel ferrites are very important magnetic materials because they have interesting magnetic and electrical properties, exhibit excellent chemical and thermal stabilities, and have high corrosion resistivity [1–4]. The spinel ferrite structure is face centered cubic close packed composed of two kinds of interstitial sites, the tetrahedral (A) and octahedral (B) sites surrounded by four and six oxygen ions, respectively [1, 2, 4]. The smaller transition metal cations (M^{2+} and Fe^{3+}) occupy the interstices of oxygen ion lattice and they are distributed in A and B sites to determine the magnetic and electronic properties of spinel ferrites [1, 2]. For example, Fe^{3+} ions are located in the tetrahedral (A) and octahedral (B) sites and Ni^{2+} ions are only located in octahedral sites for inverse spinel ferrimagnetism $NiFe_2O_4$ [2, 4] while Zn^{2+} ions occupy tetrahedrally coordinated A-sites and Fe^{3+} ions locate at octahedral B-sites for cubic spinel paramagnetic $ZnFe_2O_4$ [5]. The magnetic properties of magnetic spinel ferrite nanoparticles are very different from bulk materials due to the reduction in dimension of particles, known as surface effect [1–6], expressed by surface area (S) to volume (V) ratio for spherical nanoparticles as follows

$$\frac{S}{V} \alpha \frac{1}{r} \quad (1)$$

*Corresponding authors: phuruangrat@hotmail.com

where r is the radius [6]. Sivagurunathan et al. reported the decrease of magnetization of $ZnFe_2O_4$ by increasing the particle size of $ZnFe_2O_4$ nanoparticles [7]. Liu et al. reported that $NiFe_2O_4$ nanocrystals exhibited larger coercivity than bulk $NiFe_2O_4$ material [8].

Spinel ferrite nanomaterials can be synthesized by several methods, such as solid state reaction [9, 10], sol–gel [11, 12], co-precipitation [6, 11] and pyrolysis [13]. These methods need high synthetic temperature. Thus, the particle morphology, size distribution and formation of aggregates in the spinel ferrite nanomaterials are very difficult to be controlled. An ideal synthetic method of nanomaterials should be environmentally friendly, low-energy consumption and as simple as possible. Microwave-assisted solvothermal (MS) method, a novel preparation technique, has been used to prepare the nanosized compounds because the MS method can lead to very rapid heating to the temperature of treatment, extremely rapid kinetics of crystallization by one-to-two orders of magnitude and energy saving [14–17].

In this research, MFe_2O_4 (M = Mn, Zn, Cu and Ni) nanoparticles were synthesized by MS method using $M(NO_3)_2 \cdot 6H_2O$ (M = Mn, Zn, Cu and Ni) and $Fe(NO_3)_3 \cdot 9H_2O$ as staring materials and ethylene glycol as a solvent. Phases, morphologies and magnetic properties of MFe_2O_4 (M = Mn, Zn, Cu and Ni) nanoparticles were investigated by X-ray powder diffraction (XRD), Fourier transform infrared (FTIR) spectroscopy, transmission electron microscopy (TEM) and vibrating sample magnetometer (VSM).

2. Experimental section

In a typical synthetic procedure, 0.005 mole $M(NO_3)_2 \cdot 6H_2O$ (M = Mn, Zn, Cu and Ni) and 0.01 mole $Fe(NO_3)_3 \cdot 9H_2O$ were dissolved in 40 ml ethylene glycol under magnetic stirring until they completely dissolved. Then, the solutions were adjusted the pH to 6 by 3 M NaOH dropping. The resultant solutions were loaded and sealed in each of the 100 ml of TFM® Fluoropolymer vessel liner. The microwave reactors were transferred in a CEM Mars 5 microwave oven, heated by 300 W of microwave power at room temperature to 100 ^oC within 20 min and kept at this temperature for 30 min. In the end, they were cooled to room temperature. The products were collected, washed with deionized water and ethanol and dried at 80 ^oC for 24 h. The products were further characterized by X-ray powder diffraction (XRD), Fourier transform infrared (FTIR) spectroscopy, transmission electron microscopy (TEM) and vibrating sample magnetometer (VSM).

3. Results and discussion

Fig. 1a shows XRD patterns of the as-prepared MFe_2O_4 (M = Mn, Zn, Cu and Ni) samples synthesized by the microwave-assisted solvothermal reaction in ethylene glycol at 100 ^oC for 30 min. All diffraction peaks of the samples were assigned to the diffraction planes of (220), (311), (222), (400), (422) and (511) of cubic ferrite MFe_2O_4 (M = Mn, Zn, Cu and Ni) with a spinel-type structure, in good agreement with the crystallographic data of $MnFe_2O_4$ (JCPDS No. 10-0319) [18], $ZnFe_2O_4$ (JCPDS No. 79-1150) [18], $CuFe_2O_4$ (JCPDS No. 77-0010) [18] and $NiFe_2O_4$ (JCPDS No. 74-2081) [18]. The lattice parameters for cubic ferrite MFe_2O_4 (M = Mn, Zn, Cu and Ni) were estimated by the equation

$$\frac{1}{d^2} = \frac{h^2 + k^2 + l^2}{a^2} \tag{2}$$

where a is the lattice parameter and d is the interplanar space for the plane of (hkl) Miller indices [1, 4]. The values of lattice parameter (Table 1) calculated by the XRD data are in good agreement with those of the standard diffraction values. Using Scherrer's equation: $D = 0.9\lambda/\beta\cos\theta$, where D is the average crystalline size, λ is the wavelength of Cu-K_α, β is the full width at half maximum (FWHM) of the diffraction peaks, and θ is the Bragg's angle [3, 4]. The average crystallite size

(Table 1) of $MnFe_2O_4$, $ZnFe_2O_4$, $CuFe_2O_4$ and $NiFe_2O_4$ were estimated to be 30, 18, 22 and 25 nm, respectively.

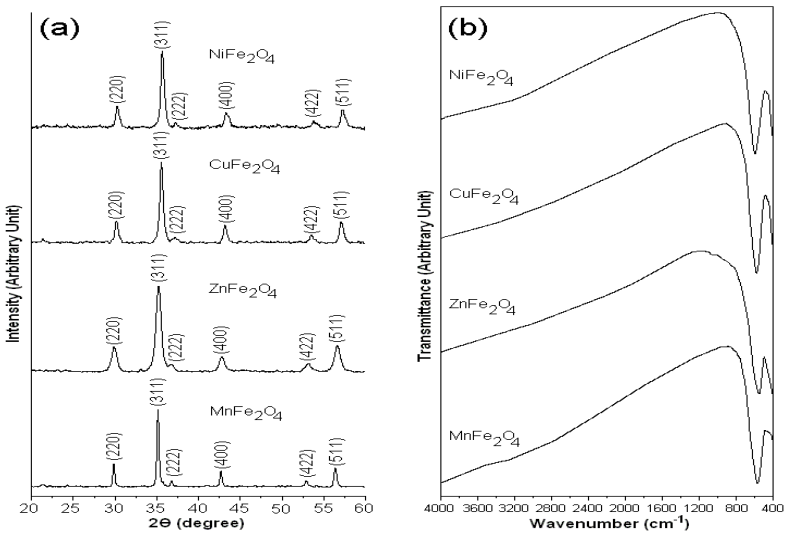

Fig. 1. (a) XRD patterns and (b) FTIR spectra of the as-prepared MFe_2O_4 (M = Mn, Zn, Cu and Ni) samples synthesized by microwave-assisted solvothermal method.

Table 1. Lattice cell, crystallite size and magnetic properties of MFe_2O_4 (M = Mn, Zn, Cu and Ni).

Sample	Calculated lattice cell (Å)	Crystallite size (nm)	H_c (Oe)	M_s (emu.g^{-1})
$MnFe_2O_4$	8.4837	30	115.08	44.95
$ZnFe_2O_4$	8.4401	18	14.72	17.07
$CuFe_2O_4$	8.3739	22	1904.20	50.98
$NiFe_2O_4$	8.3460	25	75.83	27.56

The spinal ferrite MFe_2O_4 (M = Mn, Zn, Cu and Ni) compounds have two sites, the tetrahedral (A-site) and octahedral (B-site), according to the geometrical configuration of the oxygen nearest neighbor. Two main broad metal-oxygen bands were detected in the FTIR spectra. The highest one (ν_1), generally observed in the range of 600–500 cm^{-1}, corresponds to intrinsic stretching vibration of the tetrahedral metal–oxygen stretching M_3O, $M_{tetra} \leftrightarrow O$. The ν_2-lowest one, usually observed in the range of 450–385 cm^{-1}, is assigned to octahedral metal–oxygen stretching Fe_3O, $Fe_{octa} \leftrightarrow O$ [1, 3, 4, 19]. FTIR spectra of spinel ferrite MFe_2O_4 (M = Mn, Zn, Cu and Ni) samples (Fig. 1b) show two main absorption bands at 600–400 cm^{-1}. The vibration band at ~600–585 cm^{-1} is assigned to the stretching mode of Fe–O [1, 3, 19]. The vibration band at ~407–406 cm^{-1} corresponds to the stretching mode of M–O (M = Mn, Zn, Cu and Ni) [1, 19].

Fig. 2 shows TEM images of the MFe_2O_4 (M = Mn, Zn, Cu and Ni). The TEM images of the spinal ferrite MFe_2O_4 samples exhibited well crystallized morphologies. They show MFe_2O_4 nanoparticles with less than 100 nm. Selected area electron diffraction (SAED) patterns can index to the (111), (220), (311), (400), (422), (511) and (440) planes of MFe_2O_4 (M = Mn, Zn, Cu and Ni) phases. Therefore, the spinal ferrite MFe_2O_4 (M = Mn, Zn, Cu and Ni) nanoparticles have been successful synthesized by microwave-assisted solvothermal method at 100 ^oC for 30 min. Comparing to conventional hydrothermal method, Han et al. reported the irregular flake-shaped $ZnFe_2O_4$ structure with particle size of 7–13 nm synthesized by hydrothermal method at 180 ^oC for 48 h [20]. Baykal et al. reported that the $NiFe_2O_4$ nanoparticles were synthesized by hydrothermal method at 130 ^oC for 15 h [21]. These revealed that the current method required lower synthetic

temperature, easy and energy saving because of the microwave-assisted oxide reaction provides the exothermic energy used to synthesize the spinal ferrite MFe_2O_4 (M = Mn, Zn, Cu and Ni) nanocrystals.

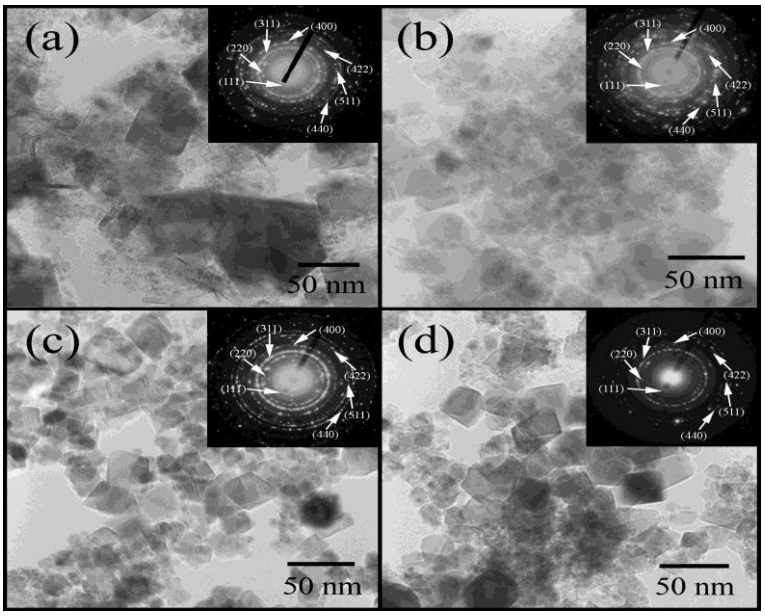

Fig. 2. TEM images and SAED patterns of the (a) $MnFe_2O_4$, (b) $ZnFe_2O_4$, (c) $CuFe_2O_4$ and (d) $NiFe_2O_4$.

Fig. 3 shows the vibrating sample magnetometer (VSM) curves of the spinel ferrite MFe_2O_4 (M = Mn, Zn, Cu and Ni) samples at room temperature. Obviously, the variation of magnetization as a function of applied field presents hysteresis loops. The observed hysteresis loops are characteristic behavior of soft magnetic materials which indicate ferromagnetic hysteresis loops in the field range of ±1000 Oe and ±3000 Oe for the $NiFe_2O_4$ and $MnFe_2O_4$ samples, respectively. The $ZnFe_2O_4$ and $CuFe_2O_4$ samples show superparamagnetic behavior [3]. The saturation magnetization (M_s) and coercive force (H_c) of MFe_2O_4 (M = Mn, Zn, Cu and Ni) nanoparticles were summarized in Table 1. They should be noted that M_s of the $NiFe_2O_4$, $MnFe_2O_4$ and $CuFe_2O_4$ nanocrystals are 27.56, 44.95 and 50.98 emu.g^{-1} which are lower than those of the corresponding bulk materials ($NiFe_2O_4$ = 55 emu.g^{-1}, $MnFe_2O_4$ = 80 emu.g^{-1} and $CuFe_2O_4$ = 74.08 emu.g^{-1}) [2, 22]. The decrease of M_s in these nanoparticles is attributed to the canted spins in the surface layer due to the decrease of the exchange coupling, caused by the lack of oxygen mediating super exchange mechanism between nearest iron ions at the surface. Comparing the M_s of $ZnFe_2O_4$ bulk (1.3 emu.g^{-1}) [23], the M_s of the current $ZnFe_2O_4$ is 17.07 emu.g^{-1} which is higher than that of the bulk due to cation inversion and smaller particle size of the $ZnFe_2O_4$ zinc ferrite nanoparticles. $ZnFe_2O_4$ shows near zero remanence and zero coercivity which could be identified as superparamagnetic materials [24, 25] because of the coupling process between cations at both octahedral and tetrahedral sites, giving rise to occurrence of superparamagnetic couple [25].

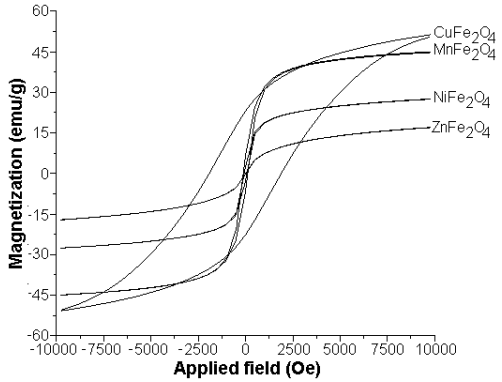

Fig. 3. M-H loops for the MFe_2O_4 (M = Mn, Zn, Cu and Ni) nanoparticles.

4. Conclusions

In summary, MFe_2O_4 (M = Mn, Zn, Cu and Ni) nanoparticles were synthesized by a microwave-assisted solvothermal method. The analytical results show that the products are cubic ferrite MFe_2O_4 (M = Mn, Zn, Cu and Ni) nanoparticles. The VSM analysis shows ferromagnetic properties for the $NiFe_2O_4$ and $MnFe_2O_4$ samples, whereas the $ZnFe_2O_4$ and $CuFe_2O_4$ samples are superparamagnetic behavior.

Acknowledgement

We are extremely grateful to Chiang Mai University for providing financial support through the Center of Excellence in Materials Science.

References

[1] D. M. Jnaneshwara, D. N. Avadhani, B. DarukaPrasad, B. M. Nagabhushana, H. Nagabhushana, S. C. Sharma, C. Shivakumara, J. L. Rao, N. O. Gopal, S. C. Ke, R. P. S. Chakradhar, J. Magn. Magn. Mater. **339**, 40 (2013).
[2] K. C. Verma, V. P. Singh, M. Ram, J. Shah, R. K. Kotnala, J. Magn. Magn. Mater. **323**, 3271 (2011).
[3] P. Sivakumar, R. Ramesh, A. Ramanand, S. Ponnusamy, C. Muthamizhchelvan, Appl. Surf. Sci. **258**, 6648 (2012).
[4] M. Kooti, A. N. Sedeh, J. Mater. Sci. Technol. **29**, 34 (2013).
[5] M. Arias, V. M. Pantojas, O. Perales, W. Otaño, J. Magn. Magn. Mater. **323**, 2109 (2011).
[6] P. A. Vinosha, L. A. Mely, J. E. Jeronsia, S. Krishnan, S. J. Das, Optik **134**, 99 (2017).
[7] P. Sivagurunathak, K. Sathiyanurthy, Canad. Chem. Transact. **4**, 244 (2016).
[8] Q. Liu, H. Huang, L. Lai, J. Sun, T. Shang, Q. Zhou, Z. Xu, J. Mater. Sci. **44**, 1187 (2009).
[9] S. Bera, A. A. M. Prince, S. Velmurugan, P.S. Raghavan, R. Gopalan, G. Pammeerselvam, S. V. Narasimhan, J. Mater. Sci. **36**, 5379 (2001).
[10] Z. Zhang, G. Yao, X. Zhang, J. Ma, H. Lin, Ceram. Inter. **41**, 4523 (2015).
[11] M. Kurian, D. S. Nair, J. Saudi Chem. Soc. **20**, S517 (2016).
[12] S. M. Masoudpanah, S. A. S. Ebrahimi, M. Derakhshani, S. M. Mirkazemi, J. Magn. Magn. Mater. **370**, 122 (2014).
[13] Z. Wu, M. Okuya, S. Kaneko, Thin Solid Films **385**, 109 (2001).
[14] K. Ocakoglu, S. A. Mansour, S. Yildirimcan, A. A. Al-Ghamdi, F. El-Tantawy, F. Yakuphanoglu, Spectrochim. Acta A **148**, 362 (2015).
[15] S. Preda, M. Rutar, P. Umek, M. Zaharescu, Mater. Res. Bull. **71**, 98 (2015).
[16] F. Bondioli, A. B. Corradi, A. M. Ferrari, C. Leonelli, J. Am. Ceram. Soc. **91**, 3746 (2008).

[17] J. Z. Marinho, L. M. Santos, L. R. Macario, E. Longo, A. E. H. Machado, A. O. T. Patrocinio, R. C. Lima, J. Braz. Chem. Soc. **26**, 498 (2015).
[18] Powder Diffract. File, JCPDS Internat. Centre Diffract. Data, PA 19073–3273 U.S.A. (2001).
[19] Y. Köseoğlu, A. Baykal, M. S. Toprak, F. Gözüak, A. C. Başaran, B. Aktaş, J. Alloy. Compd. **462**, 209 (2008).
[20] L. Han, X. Zhou, L. Wan, Y. Deng, S. Zhan, J. Environ. Chem. Eng. **2**, 123 (2014).
[21] A. Baykal, N. Kasapoğlu, Y. Köseoğlu, M. S. Toprak, H. Bayrakdar, J. Alloy. Compd. **464**, 514 (2008).
[21] M. G. Naseri, E. B. Saion, A. Kamali, ISRN Nanotechnology, **2012**, 1 (2012) Article ID 604241.
[22] M. Arias, V. M. Pantojas, O. Perales, W. Otaño, J. Magn. Magn. Mater. **323**, 2109 (2011).
[23] R. Liu, M. Lv, Q. Wang, H. Li, P. Guo, X. S. Zhao, J. Magn. Magn. Mater. **424**, 155 (2017).
[24] M. Dhiman, R. Sharma, V. Kumar, S. Singhal, Ceram. Inter. **42**, 12594 (2016).